

## 4 **Mitochondrial respiratory states and rates**

5  
6 Gnaiger Erich et al (MitoEAGLE Task Group)\*

7  
8 Corresponding author: Erich Gnaiger

9 *Chair COST Action CA15203 MitoEAGLE – <http://www.mitoeagle.org>*

10 *Department of Visceral, Transplant and Thoracic Surgery, D. Swarovski Research Laboratory,*

11 *Medical University of Innsbruck, Innrain 66/4, A-6020 Innsbruck, Austria*

12 *Email: [mitoeagle@i-med.ac.at](mailto:mitoeagle@i-med.ac.at); Tel: +43 512 566796, Fax: +43 512 566796 20*

13  
14 Running title: Mitochondrial states and rates

15  
16 **As the knowledge base and importance of mitochondrial physiology to evolution, health, and**  
17 **disease expands, the necessity for harmonizing the terminology concerning mitochondrial**  
18 **respiratory states and rates has become increasingly apparent. The chemiosmotic theory**  
19 **establishes the mechanism of energy transformation in oxidative phosphorylation (OXPHOS) and**  
20 **provides the theoretical foundation of mitochondrial physiology and bioenergetics. We follow**  
21 **guidelines of the International Union of Pure and Applied Chemistry (IUPAC) on terminology,**  
22 **extended by considerations of mitochondrial respiratory control, metabolic flows and fluxes. The**  
23 **OXPHOS-capacity is respiration measured at kinetically-saturating concentrations of ADP and**  
24 **inorganic phosphate. The oxidative electron transfer-capacity reveals the possible limitation of**  
25 **OXPHOS-capacity mediated by the phosphorylation-pathway and is measured as noncoupled**  
26 **respiration at optimum concentrations of external uncouplers. LEAK-respiration is the**  
27 **intrinsically uncoupled oxygen consumption, compensating mainly for ion leaks — particularly**  
28 **the proton leak — and studied in the absence of ADP or by inhibition of the phosphorylation-**  
29 **pathway. Uniform standards for evaluation of respiratory states and rates will ultimately**  
30 **contribute to reproducibility between laboratories and thus support the development of databases**  
31 **of mitochondrial respiratory function in species, tissues, and cell types. Clarity of concept and**  
32 **consistency of nomenclature facilitate effective transdisciplinary communication, education, and**  
33 **ultimately further discovery.**

34  
35 *Keywords:* Mitochondrial respiratory control, coupling control; mitochondrial preparations;  
36 protonmotive force; uncoupling; oxidative phosphorylation: OXPHOS; electron transfer: ET; electron  
37 transfer system: ETS; proton leak, ion leak and slip compensatory state: LEAK; residual oxygen  
38 consumption: ROX; State 2; State 3; State 4; normalization; flow; flux; oxygen: O<sub>2</sub>

### 39 40 41 **Harmonization of nomenclature**

42  
43 Mitochondria are essential cellular, membrane-enclosed organelles that perform a large range of  
44 functions critical for cell viability. Their best-known function is to synthesize adenosine triphosphate  
45 (ATP) via oxidative phosphorylation (OXPHOS), but they also have important functions related to  
46 cellular metabolism and cell-signalling. This importance has led to a large and increasing body of  
47 research devoted to better understanding mitochondrial respiratory function. However, the  
48 dissemination of fundamental knowledge and implementation of novel discoveries require  
49 communication with a commonly understood terminology. Reproducibility of experimental procedures  
50 also depends on strictly-defined conditions and harmonization of shared research protocols.  
51 Unfortunately, a consensus on nomenclature and conceptual coherence is currently missing in the  
52 expanding field of mitochondrial physiology and bioenergetics. The use of sometimes vague,  
53 ambiguous, or inconsistent terminology likely contributes to confusion, miscommunication, and the

54 conversion of valuable signals to wasteful noise. Thus, complementary to quality control a conceptual  
 55 framework is required to standardise and harmonise terminology and methodology.

56 To fill the current gap, this perspective aims to harmonize nomenclature and addresses the  
 57 terminology on coupling states and fluxes through metabolic pathways of aerobic energy transformation  
 58 in mitochondrial (mt) preparations. In an attempt to establish a transdisciplinary nomenclature, we  
 59 strive to incorporate a concept-driven terminology of bioenergetics with explicit, easily recognized  
 60 terms and symbols that define mitochondrial respiratory states and rates. The consistent use of terms  
 61 and symbols will facilitate transdisciplinary communication for quantitative modelling and data  
 62 repositories on bioenergetics and mitochondrial physiology.<sup>1-3</sup>

## 64 Coupling in mitochondrial respiration

66 **Respiration and fermentation.** Aerobic respiration is the O<sub>2</sub> flux in (1) OXPHOS with catabolic  
 67 reactions leading to O<sub>2</sub> consumption coupled to phosphorylation of ADP to ATP, plus (2) O<sub>2</sub> consuming  
 68 reactions apart from OXPHOS. Coupling of electron transfer (ET) to ADP→ATP phosphorylation is  
 69 mediated by vectorial translocation of protons across the mitochondrial inner membrane (mtIM). Proton  
 70 pumps generate or utilize the electrochemical protonmotive force, *pmF* (Fig. 1). The *pmF* is the sum of  
 71 two partial forces, the electric force (electric potential difference) and chemical force (proton chemical  
 72 potential difference, related to ΔpH).<sup>4,5</sup> Cell respiration is thus distinguished from fermentation: (1)  
 73 Compartmental coupling in vectorial OXPHOS<sup>4,5</sup> contrasts to substrate-level phosphorylation in  
 74 fermentation without utilization of O<sub>2</sub>. (2) Redox balance is maintained in aerobic respiration by O<sub>2</sub> as  
 75 the electron acceptor supplied externally, whereas fermentation is characterized by internal electron  
 76 acceptors formed in intermediary metabolism (Fig. 1a).

78 **Respiratory states and respiratory capacity.** Cell membranes include organellar membranes and the  
 79 plasma membrane, which separates the intracellular milieu from the extracellular environment (Fig. 1a).  
 80 The plasma membrane consists of a lipid bilayer with embedded proteins and attached organic  
 81 molecules that collectively control the selective permeability of ions, organic molecules and particles,  
 82 limiting the passage of many water-soluble mitochondrial substrates and inorganic ions. Such limitations  
 83 are overcome in mitochondrial preparations: plasma membranes are removed or selectively  
 84 permeabilized, while mitochondrial structural and functional integrity is maintained<sup>6</sup>. In mt-  
 85 preparations, extramitochondrial concentrations of fuel substrates, ADP, ATP, inorganic phosphate (P<sub>i</sub>),  
 86 and cations including H<sup>+</sup> can be controlled to determine mitochondrial respiratory function under a set  
 87 of conditions defined as coupling control states (Tab. 1). In substrate-uncoupler-inhibitor titration  
 88 (SUIT) protocols, substrate combinations and specific inhibitors of ET-pathway enzymes are used to  
 89 obtain defined pathway control states<sup>7,8</sup> (Fig. 1b). Pathway and coupling control states are  
 90 complementary, since mt-preparations depend on (1) an exogenous supply of pathway-specific fuel  
 91 substrates and O<sub>2</sub>, and (2) exogenous control of phosphorylation<sup>9</sup>.

92 Reference respiratory states are established with kinetically-saturating substrate concentrations  
 93 for analysis of mitochondrial respiratory capacities. These delineate — comparable to channel capacity  
 94 in information theory<sup>10</sup> — the upper boundary of O<sub>2</sub> consumption rates. Intracellular conditions in living  
 95 cells deviate from these experimental states. Further information is obtained in kinetic studies of flux as  
 96 a function of fuel substrate concentration, [ADP], or [O<sub>2</sub>] in the range between kinetically-saturating  
 97 concentrations and anoxia<sup>11</sup>.

99 **Phosphorylation.** The term phosphorylation is used generally in many contexts, *e.g.*, protein  
 100 phosphorylation. Phosphorylation in the context of OXPHOS is defined as phosphorylation of ADP by  
 101 P<sub>i</sub> to form ATP, coupled to oxidative electron transfer (Fig. 1c,d). The ET- and phosphorylation-  
 102 pathways comprise coupled components of the OXPHOS-system. P/O is the ratio of P<sub>i</sub> to atomic oxygen  
 103 consumed<sup>9</sup>. The symbol, P», is introduced here as more discriminating and specific than P (Fig. 1c).  
 104 The symbol P» indicates the endergonic (uphill) direction ADP→ATP, and likewise P« the  
 105 corresponding exergonic (downhill) hydrolysis ATP→ADP (Fig. 2). *J<sub>P»</sub>* and *J<sub>P«</sub>* are the corresponding  
 106 fluxes of ADP phosphorylation and ATP hydrolysis, respectively. P» refers mainly to phosphorylation  
 107 driven by proton translocation (Fig. 1d),<sup>12</sup> but may also involve substrate-level phosphorylation in the  
 108 mitochondrial matrix (succinyl-CoA ligase, monofunctional C1-tetrahydrofolate synthase), cytosol  
 109 (phosphoglycerate kinase and pyruvate kinase), or both (phosphoenolpyruvate carboxykinase isoforms

110 1 and 2). Kinase cycles are involved in intracellular energy transfer and signal transduction for regulation  
 111 of energy flux <sup>13</sup>.

112

## 113 **Respiratory coupling control states: concept and nomenclature**

114

115 **Concept-driven terminology.** Respiratory control refers to the ability of mitochondria to adjust O<sub>2</sub> flux  
 116 in response to external control signals by engaging various mechanisms of control and regulation<sup>14</sup>.  
 117 Respiratory control is monitored in mt-preparations under conditions defined as respiratory states,  
 118 preferentially under near-physiological conditions of temperature, pH, and medium ionic composition.  
 119 When phosphorylation of ADP to ATP is stimulated or depressed, an increase or decrease is observed  
 120 in electron transfer measured as O<sub>2</sub> flux in respiratory coupling states of intact mitochondria ('controlled  
 121 states' in the classical terminology of bioenergetics). Alternatively, coupling of electron transfer with  
 122 phosphorylation is diminished by uncouplers, which eliminates control by P<sub>»</sub> and increases respiratory  
 123 rate (noncoupled or 'uncontrolled state'; Tab. 1).

124 Coupling efficiency is diminished by intrinsic and extrinsic uncoupling. Uncoupling of  
 125 mitochondrial respiration is a general term comprising diverse mechanisms. Differences of terms —  
 126 uncoupled vs. noncoupled — are easily overlooked, although they relate to different meanings of  
 127 uncoupling (Tab. 2).

128 To extend the classical nomenclature on mitochondrial states (State 1 to 5) <sup>15</sup> by a concept-driven  
 129 terminology that explicitly incorporates information on the meaning of respiratory states, the  
 130 terminology must be general and not restricted to any particular experimental protocol or mitochondrial  
 131 preparation <sup>16</sup>. Standard respiratory coupling states are obtained while maintaining a defined ET-  
 132 pathway state with constant fuel substrates and inhibitors of specific branches of the ET-pathway. The  
 133 focus of concept-driven nomenclature is primarily the theoretical *why*, along with clarification of the  
 134 experimental *how* <sup>17</sup>.

135 In the three coupling states — LEAK, OXPHOS, and ET — the corresponding respiratory rates  
 136 are abbreviated as *L*, *P*, and *E*, respectively (Fig. 2a). The *pmF* is *maximum* in the LEAK-state of coupled  
 137 mitochondria, driven by LEAK-respiration at a minimum back-flux of cations to the matrix  
 138 compartment, *high* in the OXPHOS-state when it drives phosphorylation, and *low* in the ET-state when  
 139 uncouplers short-circuit the proton cycle (Tab. 1).

140

141 **LEAK-state - Fig. 2b.** The LEAK-state is the state of mitochondrial respiration when O<sub>2</sub> flux mainly  
 142 compensates for ion leaks in the absence of ATP synthesis, at kinetically-saturating concentrations of  
 143 O<sub>2</sub> and respiratory fuel substrates. Stimulation of phosphorylation is prevented by (1) absence of ADP  
 144 and ATP; (2) maximum ATP/ADP ratio (State 4); or (3) inhibition of the phosphorylation-pathway with  
 145 inhibitors of F<sub>1</sub>F<sub>0</sub>-ATPase (oligomycin; Omy) or adenine nucleotide translocase (carboxyatractyloside;  
 146 Tab. 1). The chelator EGTA is added to mt-respiration media to bind free Ca<sup>2+</sup>, thus limiting cation  
 147 cycling. LEAK-respiration is the intrinsically uncoupled O<sub>2</sub> consumption without addition of  
 148 uncouplers. The LEAK-rate is a function of respiratory state, hence it depends on (1) the barrier function  
 149 of the mtIM ('leakiness'), (2) the electrochemical potential differences and concentration differences  
 150 across the mtIM, and (3) the H<sup>+</sup>/O<sub>2</sub> ratio of the ET-pathway (Fig. 1b).

151 State 4 is a LEAK-state after depletion of ADP <sup>15</sup>. O<sub>2</sub> flux in State 4 overestimates LEAK-  
 152 respiration if ATP hydrolysis activity recycles ATP to ADP,  $J_{P«}$ , which stimulates respiration coupled  
 153 to phosphorylation,  $J_{P»} > 0$ . Inhibition of the phosphorylation-pathway by oligomycin ensures that  $J_{P»} =$   
 154 0 (State 4o; Tab. 1).

155

156 **OXPHOS-state - Fig. 2c.** At any given ET-pathway state, the OXPHOS-state establishes conditions to  
 157 measure OXPHOS-capacity as a reference, at kinetically-saturating concentrations of O<sub>2</sub>, as well as  
 158 respiratory fuel and phosphorylation substrates. Respiratory OXPHOS-capacities, *P*, are related to ADP-  
 159 phosphorylation capacities by the ATP yield per O<sub>2</sub> (Fig. 1c).

160 The OXPHOS-state is compared with State 3, which is the state stimulated by addition of fuel  
 161 substrates while the ADP concentration in the preceding State 2 (see below) is still 'high' and supports  
 162 coupled energy transformation in isolated mitochondria in a closed respirometric chamber <sup>15</sup>. Repeated  
 163 ADP titrations re-establish State 3. Starting at experimental O<sub>2</sub> concentrations,  $c_{O_2}$ , of air-saturation (193  
 164 or 238 μM O<sub>2</sub> at 37 °C or 25 °C and sea level at 1 atm or 101.32 kPa, and an oxygen solubility of  
 165 respiration medium at 0.92 times that of pure water) <sup>18</sup>, the added ADP concentrations must be low

166 enough (typically 100 to 300  $\mu\text{M}$ ) to allow phosphorylation to ATP without  $\text{O}_2$  depletion during the  
 167 transition to State 4. In contrast, kinetically-saturating ADP concentrations are usually 10-fold higher  
 168 than 'high ADP' (e.g., 2.5 mM) supporting OXPHOS capacity in isolated mitochondria<sup>11</sup>.

169  
 170 **Electron transfer-state - Fig. 2d.** The ET-state is defined as the *noncoupled* state with kinetically-  
 171 saturating concentrations of  $\text{O}_2$  and respiratory substrate, and optimum exogenous uncoupler  
 172 concentration for maximum  $\text{O}_2$  flux (ET-capacity). Uncouplers are weak lipid-soluble acids that  
 173 function as protonophores. These disrupt the barrier function of the mtIM and thus short-circuit the  
 174 protonmotive system, functioning like a clutch in a mechanical device. As a consequence of the nearly  
 175 collapsed *pmF*, the driving force is insufficient for phosphorylation and  $J_{P_s} = 0$ . The most frequently  
 176 used uncouplers are carbonyl cyanide *m*-chloro phenyl hydrazone (CCCP), carbonyl cyanide *p*-  
 177 trifluoromethoxyphenylhydrazone (FCCP), or dinitrophenol (DNP). Stepwise titration of uncouplers  
 178 stimulates respiration up to or above the level of  $\text{O}_2$  consumption rates in the OXPHOS-state; respiration  
 179 is inhibited, however, above optimum uncoupler concentrations<sup>5</sup>.

180 The abbreviation State 3u is occasionally used to indicate the state of respiration after titration of  
 181 an uncoupler, without sufficient emphasis on the fundamental difference between OXPHOS-capacity  
 182 (*well-coupled* with an endogenous uncoupled component) and ET-capacity (*noncoupled*; Fig. 2a).

183  
 184 **ROX-state versus anoxia.** The state of residual  $\text{O}_2$  consumption, ROX, is not a coupling state. The rate  
 185 of residual oxygen consumption, *Rox*, is defined as  $\text{O}_2$  consumption due to oxidative reactions measured  
 186 after inhibition of ET with antimycin A alone or in combination with rotenone and malonic acid.  
 187 Cyanide and azide inhibit not only CIV but also catalase and several peroxidases. *Rox* represents a  
 188 baseline to correct respiration: *Rox*-corrected *L*, *P* and *E* are not only lower than total fluxes, but also  
 189 change the flux control ratios *L/P* and *L/E*. *Rox* is not necessarily equivalent to non-mitochondrial  
 190 respiration, considering  $\text{O}_2$ -consuming reactions in mitochondria that are not related to ET — such as  
 191  $\text{O}_2$  consumption in reactions catalyzed by monoamine oxidases, monooxygenases (cytochrome P450  
 192 monooxygenases), dioxygenases (trimethyllysine dioxygenase), and several hydroxylases.

193 In the nomenclature of Chance and Williams, State 2 is induced by titration of ADP before  
 194 addition of fuel substrates<sup>15,19</sup>. ADP stimulates respiration transiently on the basis of endogenous fuel  
 195 substrates resulting in phosphorylation of a small portion of the added ADP. State 2 is then a ROX state  
 196 at minimum respiratory activity after exhaustion of endogenous fuel substrates. State 5 'may be obtained  
 197 by antimycin A treatment or by anaerobiosis'<sup>15</sup>. These definitions give State 5 two different meanings:  
 198 ROX or anoxia.

199 Anoxia is induced after exhaustion of  $\text{O}_2$  in a closed respirometric chamber. Diffusion of  $\text{O}_2$  from  
 200 the surroundings into the aqueous solution is a confounding factor potentially preventing complete  
 201 anoxia<sup>11</sup>.

202

## 203 Rates and SI units

204

205 The term *rate* is not adequately defined to be useful for reporting data. A rate can be (1) an extensive  
 206 quantity<sup>1</sup>, termed *flow*, *I*, when expressed per chamber (instrumental system) or per countable, non-  
 207 divisible *object* (number of cells, organisms, 'in-dividuals'); or (2) a size-specific quantity, termed *flux*,  
 208 *J*, when expressed per volume or mass<sup>2</sup> (Fig. 3).

209 Different units are used to report the  $\text{O}_2$  consumption rate, OCR. SI units provide the common  
 210 reference with appropriately chosen SI prefixes<sup>1</sup>. Although volume is expressed as  $\text{m}^3$  using the SI base  
 211 unit, the liter [ $\text{dm}^3$ ] is a conventional unit of volume for concentration and is used for most solution  
 212 chemical kinetics. Constants for conversion to SI units are summarized in Tab. 3.

213

## 214 Normalization of rate per system

215

216 **Flow: per chamber.** The instrumental system (chamber) is part of the measurement instrument,  
 217 separated from the environment as an isolated, closed, open, isothermal or non-isothermal system.  
 218 Analyses are restricted to intra-experimental comparison of relative differences, when reporting  $\text{O}_2$   
 219 flows per respiratory chamber,  $I_{\text{O}_2}$  [ $\text{nmol}\cdot\text{s}^{-1}$ ] (Fig. 3).

220

221 **Flux: per chamber volume.** System volume-specific O<sub>2</sub> flux,  $J_{V,O_2}$  (per liquid  $V$  of the instrumental  
 222 chamber [L]), is of methodological interest in relation to the instrumental limit of detection.  $J_{V,O_2}$   
 223 increases in proportion to sample concentration in the chamber. At an O<sub>2</sub> flow of 100 amol·s<sup>-1</sup>·cell<sup>-1</sup> and  
 224 a cell concentration of 10<sup>9</sup> cells·L<sup>-1</sup> (10<sup>6</sup> cells·mL<sup>-1</sup>),  $J_{V,O_2}$  is 100 nmol·s<sup>-1</sup>·L<sup>-1</sup> (100 pmol·s<sup>-1</sup>·mL<sup>-1</sup>).  $J_{V,O_2}$   
 225 should be independent of the chamber volume at constant sample concentration. There are practical  
 226 limitations to increasing the sample concentration in the chamber, when one is concerned about  
 227 crowding effects and instrumental time resolution.

228

## 229 Normalization of rate per sample

230

231 **Flow: per object.** The oxygen flow per countable object,  $I_{O_2/NX}$ , is  $I_{O_2}$  divided by the number of objects  
 232 in the chamber,  $N_X$  [x]. The oxygen flow per cell,  $I_{O_2/N_{ce}}$ , is obtained from volume-specific O<sub>2</sub> flux,  $J_{V,O_2}$   
 233 [nmol·s<sup>-1</sup>·L<sup>-1</sup>], divided by the number concentration of cells,  $C_{N_{ce}}$  [x·L<sup>-1</sup>].  $C_{N_{ce}} = N_{ce}·V^{-1}$ , where  $N_{ce}$  is the  
 234 number of cells in the chamber. O<sub>2</sub> flow is expressed in units of attomole (10<sup>-18</sup> mol) of O<sub>2</sub> consumed  
 235 per second per cell [amol·s<sup>-1</sup>·cell<sup>-1</sup>]<sup>20</sup>, numerically equivalent to [pmol·s<sup>-1</sup>·10<sup>-6</sup> cells]. Generally,  $C_{NX}$  is  
 236 the experimental number concentration of sample  $X$ . Several sample types are not countable objects,  
 237 *e.g.*, tissue homogenate, in which case a sample-specific oxygen flow cannot be expressed.

238

239 **Size-specific flux: per sample size.** Mass-specific flux,  $J_{O_2/mX}$  [mol·s<sup>-1</sup>·kg<sup>-1</sup>], expresses respiration  
 240 normalized per mass of the sample. Mass-specific oxygen flux integrates the quality and density of  
 241 mitochondria, and thus provides the appropriate normalization for evaluation of tissue performance.  
 242 When studying isolated mitochondria and homogenized or permeabilized tissues and cells,  $J_{O_2/mX}$  should  
 243 be independent of the mass-concentration of the subsample obtained from the same tissue or cell culture.  
 244  $I_{O_2/N_{ce}}$  can be directly compared only between cells of identical size. To take into account differences in  
 245 cell size, normalization is required to obtain cell size-specific flux,  $J_{O_2/m_{ce}}$  or  $J_{O_2/V_{ce}}$ <sup>21</sup> (Fig. 3).

246

247 **Marker-specific flux: per mitochondrial content.** To evaluate differences in mitochondrial respiration  
 248 independent of mitochondrial density, flux is normalized for structural or functional mt-elementary  
 249 markers, *mtE*, expressed in marker-specific mt-elementary units [mtEU] (Fig. 3). For example, citrate  
 250 synthase (CS) activity is a frequently applied functional *mtE* expressed in international units, IU  
 251 [μmol·min<sup>-1</sup>] (1 IU of CS forms 1 μmol of citrate per min; although the SI unit [nmol·s<sup>-1</sup>] would be  
 252 preferable). Then the mtEU is taken as [μmol·min<sup>-1</sup>] or [nmol·s<sup>-1</sup>]. Volume-specific oxygen flux,  $J_{V,O_2}$   
 253 [pmol·s<sup>-1</sup>·mL<sup>-1</sup>], is divided by CS activity expressed per chamber volume [mtEU·mL<sup>-1</sup>], to obtain marker-  
 254 specific respiratory flux,  $J_{O_2/mtE}$  [pmol·s<sup>-1</sup>·mtEU<sup>-1</sup>]. Alternatively,  $J_{O_2/mtE}$  is calculated from tissue mass-  
 255 specific flux of permeabilized muscle fibers,  $J_{O_2/m}$  [pmol O<sub>2</sub>·s<sup>-1</sup>·mg<sup>-1</sup>], divided by tissue mass-specific  
 256 CS activity [mtEU·mg<sup>-1</sup>].  $J_{O_2/mtE}$  is independent of mitochondrial density. If the respirometric and  
 257 enzymatic assays are performed at an identical temperature, OXPHOS- or ET-capacity can be compared  
 258 with the capacity of CS as a regulatory enzyme in the tricarboxylic acid (TCA) cycle, which is of interest  
 259 in the context of metabolic flux control.

260

261 One cannot assume that quantitative changes in various markers — such as CS activity, other  
 262 mitochondrial enzyme activities or protein content — necessarily occur in parallel with one another<sup>22</sup>.  
 263 It should be established that the marker chosen is not selectively altered by the compared trait or  
 264 treatment. In conclusion, the normalization must reflect the question under investigation. On the other  
 265 hand, the goal of combining results across projects and institutions requires standardization of  
 normalization for entry into a databank.

266

267 Comparable to the concept of the respiratory acceptor control ratio,  $RCR = \text{State 3}/\text{State 4}$ ,<sup>9</sup> the  
 268 most readily applied normalization is that of flux control ratios and flux control factors<sup>8,16</sup>. Then, instead  
 269 of a specific mt-enzyme activity, the respiratory activity in a reference state serves as the *mtE*, yielding  
 270 a dimensionless ratio of two fluxes measured consecutively in the same respirometric titration protocol.  
 271 Selection of the state of maximum flux in a protocol as the reference state — *e.g.*, ET-state in *L/E* and  
 272 *P/E* flux control ratios<sup>16</sup> — has the advantages of: (1) elimination of experimental variability in  
 273 additional measurements, such as determination of enzyme activity or tissue mass; (2) statistically  
 274 validated linearization of the response in the range of 0 to 1; and (3) consideration of maximum flux for  
 275 integrating a large number of metabolic steps in the OXPHOS- or ET-pathways. This reduces the risk  
 of selecting a functional marker that is specifically altered by the treatment or pathology, yet increases



276 the chance that the highly integrative pathway is affected, *e.g.*, the OXPHOS- rather than ET-pathway  
 277 in case of an enzymatic defect in the phosphorylation-pathway. In this case, additional information can  
 278 be obtained by reporting flux control ratios based on a reference state that indicates stable tissue mass-  
 279 specific flux.  
 280

## 281 Conclusions

282  
 283 Clarity of concepts on mitochondrial respiratory control can serve as a gateway to better diagnose  
 284 mitochondrial respiratory adaptations and defects linked to genetic variation, age-related health risks,  
 285 sex-specific mitochondrial performance, lifestyle with its effects on degenerative diseases, and thermal  
 286 and chemical environment. The challenges of measuring mitochondrial respiratory flux are matched by  
 287 those of normalization: We distinguish between (1) the instrumental *system* or *chamber* with volume  $V$   
 288 and mass  $m$  defined by the system boundaries, and (2) the *sample* or *objects* with volume  $V_X$  and mass  
 289  $m_X$  that are enclosed in the instrumental chamber. Metabolic  $O_2$  flow per countable object increases as  
 290 the size of the object is increased. This confounding factor is eliminated by expressing respiration as  
 291 mass-specific or cell volume-specific  $O_2$  flux. The present recommendations on coupling control states  
 292 and respiratory rates are focused on studies using mitochondrial preparations. Terms and symbols are  
 293 summarized in Tab. 4. These need to be complemented by considerations on pathway control of  
 294 mitochondrial respiration<sup>7,8,23</sup>, respiratory states and rates in living cells, respiratory flux control ratios,  
 295 and harmonization of experimental procedures. The present perspective is extended in a more detailed  
 296 overview on quantitative mitochondrial physiology<sup>24</sup>.  
 297

## 298 References

- 299  
 300 1. Cohen, E. R. et al. *IUPAC Green Book, 3rd Edition, 2nd Printing, IUPAC & RSC Publishing, Cambridge*  
 301 (2008).  
 302 2. Gnaiger, E. *Pure Appl Chem* **65**, 1983-2002 (1993).  
 303 3. Beard, D. A. *PLoS Comput Biol* **1**, e36 (2005).  
 304 4. Mitchell, P. *Nature* **191**, 144-148 (1961).  
 305 5. Mitchell, P. *Biochim Biophys Acta Bioenergetics* **1807**, 1507-1538 (2011).  
 306 6. Schmitt, S. et al. *Anal Biochem* **443**, 66-74 (2013).  
 307 7. Doerrier, C. et al. *Methods Mol Biol* **1782**, 31-70 (2018).  
 308 8. §Gnaiger, E. *Bioenerg Commun* **2020.2**, doi:10.26124/bec:2020-0002.v1 (2020).  
 309 9. Chance, B. & Williams, G. R. *J Biol Chem* **217**, 383-393 (1955).  
 310 10. Schneider, T. D. *IEEE Eng Med Biol Mag* **25**, 30-33 (2006).  
 311 11. Gnaiger, E. *Respir Physiol* **128**, 277-297 (2001).  
 312 12. Watt, I. N. et al. *Proc Natl Acad Sci U S A* **107**, 16823-16827 (2010).  
 313 13. Németh, B. et al. *FASEB J* **30**, 286-300 (2016).  
 314 14. Fell, D. *Understanding the control of metabolism. Portland Press* (1997).  
 315 15. Chance, B. & Williams, G. R. *J Biol Chem* **217**, 409-427 (1955).  
 316 16. Gnaiger, E. *Int J Biochem Cell Biol* **41**, 1837-1845 (2009).  
 317 17. Miller, G. A. *The science of words. Scientific American Library New York* (1991).  
 318 18. Forstner, H. & Gnaiger, E. In: *Polarographic Oxygen Sensors. Aquatic and Physiological Applications.*  
 319 *Gnaiger, E. & Forstner, H. (eds), Springer, Berlin, Heidelberg, New York*, 321-333 (1983).  
 320 19. Chance, B. & Williams, G. R. *Adv Enzymol Relat Subj Biochem* **17**, 65-134 (1956).  
 321 20. Wagner, B. A., Venkataraman, S. & Buettner, G. R. *Free Radic Biol Med* **51**, 700-712 (2011).  
 322 21. Renner, K. et al. *Biochim Biophys Acta* **1642**, 115-123 (2003).  
 323 22. Drahotka, Z. et al. *Physiol Res* **53**, 119-122 (2004).  
 324 23. Schöpf, B. et al. *Nat Commun* **11**, 1487 (2020).  
 325 24. §Gnaiger, E. et al. *Bioenerg Commun* **2020.1**, doi:10.26124/bec:2020-0001.v1 (2020).  
 326 25. Canton, M. et al. *Biochem J* **310**, 477-481 (1995).  
 327 26. Rich, P. R. *Encyclopedia Biol Chem* **1**, 467-472 (2013).  
 328 27. Lemieux, H., Blier, P. U. & Gnaiger, E. *Sci Rep* **7**, 2840 (2017).  
 329

330 § To be released with DOI until acceptance by *Nat Metab*

331 At present:

- 332 8. Gnaiger, E. *Mitochondr Physiol Network 19.12. Oroboros MiPNet Publications, Innsbruck* (2014).  
 333 24. Gnaiger, E. et al. *MitoFit Preprint Arch* doi:10.26124/mitofit:190001.v6 (2019).  
 334

335 **\*Authors (MitoEAGLE Task Group):** Gnaiger Erich, Aasander Frostner Eleonor, Abdul Karim  
336 Norwahidah, Abdel-Rahman Engy Ali, Abumrad Nada A, Acuna-Castroviejo Dario, Adiele Reginald  
337 C, Ahn Bumsoo, Alencar Mayke Bezerra, Ali Sameh S, Almeida Angeles, Alton Lesley, Alves Marco  
338 G, Amati Francesca, Amoedo Nivea Dias, Amorim Ricardo, Anderson Ethan J, Andreadou Ioanna,  
339 Antunes Diana, Arago Marc, Aral Cenk, Arandarcikaite Odeta, Arias-Reyes Christian, Armand Anne-  
340 Sophie, Arnould Thierry, Avram Vlad F, Axelrod Christopher L, Bailey Damian M, Bairam Aida,  
341 Bajpeyi Sudip, Bajzikova Martina, Bakker Barbara M, Banni Aml, Bardal Tora, Barlow J, Bastos  
342 Sant'Anna Silva Ana Carolina, Batterson Philip M, Battino Maurizio, Bazil Jason N, Beard Daniel A,  
343 Bednarczyk Piotr, Beleza Jorge, Bello Fiona, Ben-Shachar Dorit, Bento Guida Jose Freitas, Bergdahl  
344 Andreas, Berge Rolf K, Bergmeister Lisa, Bernardi Paolo, Berridge Michael V, Bettinazzi Stefano,  
345 Bishop David J, Blier Pierre U, Blindheim Dan Filip, Boardman Neoma T, Boetker Hans Erik, Borchard  
346 Sabine, Boros Mihaly, Boersheim Elisabet, Borrás Consuelo, Borutaite Vilma, Botella Javier, Bouillaud  
347 Frederic, Bouitbir Jamal, Boushel Robert C, Bovard Josh, Bravo-Sagua Roberto, Breton Sophie, Brown  
348 David A, Brown Guy C, Brown Robert Andrew, Brozinick Joseph T, Buettner Garry R, Burtscher  
349 Johannes, Calabria Elisa, Calbet Jose AL, Calzia Enrico, Cannon Daniel T, Cano Sanchez Maria  
350 Consolacion, Canto Alvarez Carles, Cardinale Daniele A, Cardoso Luiza HD, Carvalho Eugenia,  
351 Casado Pinna Marta, Cassar Samantha, Castelo Rueda Maria Paulina, Castilho Roger F, Cavalcanti-de-  
352 Albuquerque Joao Paulo, Cecatto Cristiane, Celen Murat C, Cervinkova Zuzana, Chabi Beatrice,  
353 Chakrabarti Lisa, Chakrabarti Sasanka, Chaurasia Bhagirath, Chen Quan, Chicco Adam J, Chinopoulos  
354 Christos, Chowdhury Subir Kumar, Cizmarova Beata, Clementi Emilio, Coen Paul M, Cohen Bruce H,  
355 Coker Robert H, Collin-Chenot Anne, Coughlan Melinda T, Coxito Pedro, Crisostomo Luis, Crispim  
356 Marcell, Crossland Hannah, Dahdah Norma Ramon, Dalgaard Louise T, Dambrova Maija, Danhelovska  
357 Tereza, Darveau Charles-A, Darwin Paula M, Das Anibh Martin, Dash Ranjan K, Davidova Eliska,  
358 Davis Michael S, De Bem Andreza Fabro, De Goede Paul, De Palma Clara, De Pinto Vito, Dela  
359 Flemming, Dembinska-Kiec Aldona, Detraux Damian, Devaux Yvan, Di Marcello Marco, Di Paola  
360 Floriana Jessica, Dias Candida, Dias Tania R, Diederich Marc, Distefano Giovanna, Djafarzadeh  
361 Siamak, Doermann Niklas, Doerrier Carolina, Dong Lan-Feng, Donnelly Chris, Drahota Zdenek, Duarte  
362 Filipe Valente, Dubouchaud Herve, Duchen Michael R, Dumas Jean-Francois, Durham William J,  
363 Dymkowska Dorota, Dyrstad Sissel E, Dyson Alex, Dzialowski Edward M, Eaton Simon, Ehinger  
364 Johannes K, Elmer Eskil, Endlicher Rene, Engin Ayse Basak, Escames Germaine, Evinova Andrea,  
365 Ezrova Zuzana, Falk Marni J, Fell David A, Ferdinandy Peter, Ferko Miroslav, Fernandez-Vizarra  
366 Erika, Ferreira Julio Cesar B, Ferreira Rita Maria P, Ferri Alessandra, Fessel Joshua Patrick, Festuccia  
367 William T, Filipovska Aleksandra, Fisar Zdenek, Fischer Christine, Fischer Michael J, Fisher Gordon,  
368 Fisher Joshua J, Fontanesi Flavia, Ford Ellen, Fornaro Mara, Fuertes Agudo Marina, Fulton Montana,  
369 Galina Antonio, Galkin Alexander, Gallee Leon, Galli Gina L J, Gama Perez Pau, Gan Zhenji, Ganetzky  
370 Rebecca, Gao Yun, Garcia Geovana S, Garcia-Rivas Gerardo, Garcia-Roves Pablo Miguel, Garcia-  
371 Souza Luiz F, Garlid Keith D, Garrabou Gloria, Garten Antje, Gastaldelli Amalia, Gayen Jiaur, Genders  
372 Amanda J, Genova Maria Luisa, Giampieri Francesca, Giovarelli Matteo, Glatz Jan FC, Goikoetxea  
373 Usandizaga Naroa, Goncalo Teixeira da Silva Rui, Goncalves Debora Farina, Gonzalez-Armenta Jenny  
374 L, Gonzalez-Franquesa Alba, Gonzalez-Freire Marta, Gonzalo Hugo, Goodpaster Bret H, Gorr Thomas  
375 A, Gourlay Campbell W, Grams Bente, Granata Cesare, Grefte Sander, Grilo Luis, Guarch Meritxell  
376 Espino, Gueguen Naig, Gumeni Sentiljana, Haas Clarissa, Haavik Jan, Hachmo Yafit, Haendeler Judith,  
377 Haider Markus, Hajrulahovic Anesa, Hamann Andrea, Han Jin, Han Woo Hyun, Hancock Chad R, Hand  
378 Steven C, Handl Jiri, Hansikova Hana, Hardee Justin P, Hargreaves Iain P, Harper Mary-Ellen, Harrison  
379 David K, Hassan Hazirah, Hatokova Zuzana, Hausenloy Derek J, Heales Simon JR, Hecker Matthias,  
380 Heiestad Christina, Hellgren Kim T, Henrique Alexandrino, Hepple Russell T, Hernansanz-Agustin  
381 Pablo, Hewakapuge Sudinna, Hickey Anthony J, Ho Dieu Hien, Hoehn Kyle L, Hoel Fredrik, Holland  
382 Olivia J, Holloway Graham P, Holzner Lorenz, Hoppel Charles L, Hoppel Florian, Hoppeler Hans,  
383 Houstek Josef, Huete-Ortega Maria, Hyrossova Petra, Iglesias-Gonzalez Javier, Irving Brian A, Isola  
384 Raffaella, Iyer Shilpa, Jackson Christopher Benjamin, Jadiya Pooja, Jana Prado Fabian, Jandeleit-Dahm  
385 Karin, Jang David H, Jang Young Charles, Janowska Joanna, Jansen Kirsten M, Jansen-Duerr Pidder,  
386 Jansone Baiba, Jarmuszkiewicz Wieslawa, Jaskiewicz Anna, Jaspers Richard T, Jedlicka Jan, Jerome  
387 Estaquier, Jespersen Nichlas Riise, Jha Rajan Kumar, Jones John G, Joseph Vincent, Jurczak Michael  
388 J, Jurk Diana, Jusic Amela, Kaambre Tuuli, Kaczor Jan Jacek, Kainulainen Heikki, Kampa Rafal Pawel,  
389 Kandel Sunil Mani, Kane Daniel A, Kapferer Werner, Kapnick Senta, Kappler Lisa, Karabatsiakis  
390 Alexander, Karavaeva Iuliia, Karkucinska-Wieckowska Agnieszka, Kaur Sarbjot, Keijer Jaap, Keller

391 Markus A, Keppner Gloria, Khamoui Andy V, Kidere Dita, Kilbaugh Todd, Kim Hyoung Kyu, Kim  
392 Julian KS, Kimoloi Sammy, Klepinin Aleksandr, Klepinina Lyudmila, Klingenspor Martin, Klocker  
393 Helmut, Kolassa Iris, Komlodi Timea, Koopman Werner JH, Kopitar-Jerala Natasa, Kowaltowski Alicia  
394 J, Kozlov Andrey V, Krajcova Adela, Krako Jakovljevic Nina, Kristal Bruce S, Krycer James R, Kuang  
395 Jujiao, Kucera Otto, Kuka Janis, Kwak Hyo Bum, Kwast Kurt E, Kwon Oh Sung, Laasmaa Martin,  
396 Labieniec-Watala Magdalena, Lagarrigue Sylviane, Lai Nicola, Lalic Nebojsa M, Land John M, Lane  
397 Nick, Laner Verena, Lanza Ian R, Laouafa Sofien, Laranjinha Joao, Larsen Steen, Larsen Terje S,  
398 Lavery Gareth G, Lazou Antigone, Ledo Ana Margarida, Lee Hong Kyu, Leeuwenburgh Christiaan,  
399 Lehti Maarit, Lemieux Helene, Lenaz Giorgio, Lerfall Joergen, Li Pingan Andy, Li Puma Lance, Liang  
400 Liping, Liepins Edgars, Lin Chien-Te, Liu Jiankang, Lopez Garcia Luis Carlos, Lucchinetti Eliana, Ma  
401 Tao, Macedo Maria Paula, Machado Ivo F, Maciej Sarah, MacMillan-Crow Lee Ann, Magalhaes Jose,  
402 Magri Andrea, Majtnerova Pavlina, Makarova Elina, Makrecka-Kuka Marina, Malik Afshan N,  
403 Marcouiller Francois, Markova Michaela, Markovic Ivanka, Martin Daniel S, Martins Ana Dias,  
404 Martins Joao D, Maseko Tumisang Edward, Maull Felicia, Mazat Jean-Pierre, McKenna Helen T,  
405 McKenzie Matthew, Mendham Amy, Menze Michael A, Mercer John R, Merz Tamara, Messina  
406 Angelina, Meszaros Andras, Methner Axel, Michalak Slawomir, Mila Guasch Maria, Minuzzi Luciele  
407 M, Moellering Douglas R, Moiso Nicoleta, Molina Anthony JA, Montaigne David, Moore Anthony L,  
408 Moore Christy, Moreau Kerrie, Moreira Bruno P, Moreno-Sanchez Rafael, Mracek Tomas, Muccini  
409 Anna Maria, Munro Daniel, Muntane Jordi, Muntean Danina M, Murray Andrew James, Musiol Eva,  
410 Nabben Miranda, Nair K Sreekumaran, Nehlin Jan O, Nemeč Michal, Nesci Salvatore, Neuffer P Darrell,  
411 Neuzil Jiri, Nevier Remi, Newsom Sean A, Norman Jennifer, Nozickova Katerina, Nunes Sara, O'Brien  
412 Kristin, O'Brien Katie A, O'Gorman Donal, Olgar Yusuf, Oliveira Ben, Oliveira Jorge, Oliveira Marcus  
413 F, Oliveira Marcos Tulio, Oliveira Pedro Fontes, Oliveira Paulo J, Olsen Rolf Erik, Orynbayeva Zulfiya,  
414 Osiewacz Heinz D, Paez Hector, Pak Youngmi Kim, Pallotta Maria Luigia, Palmeira Carlos, Parajuli  
415 Nirmala, Passos Joao F, Passrigger Manuela, Patel Hemal H, Pavlova Nadia, Pavlovic Kasja, Pecina  
416 Petr, Pedersen Tina M, Perales Jose Carles, Pereira da Silva Grilo da Silva Filomena, Pereira Rita,  
417 Pereira Susana P, Perez Valencia Juan Alberto, Perks Kara L, Pesta Dominik, Petit Patrice X, Pettersen  
418 Nitschke Ina Katrine, Pichaud Nicolas, Pichler Irene, Piel Sarah, Pietka Terri A, Pinho Sonia A, Pino  
419 Maria F, Pirkmajer Sergej, Place Nicolas, Plangger Mario, Porter Craig, Porter Richard K, Pregoica  
420 Ines, Prigione Alessandro, Procaccio Vincent, Prochownik Edward V, Prola Alexandre, Pulinilkunnil  
421 Thomas, Puskarich Michael A, Puurand Marju, Radenkovic Filip, Ramzan Rabia, Rattan Suresh IS,  
422 Reano Simone, Reboredo-Rodriguez Patricia, Rees Bernard B, Renner-Sattler Kathrin, Rial Eduardo,  
423 Robinson Matthew M, Roden Michael, Rodrigues Ana Sofia, Rodriguez Enrique, Rodriguez-Enriquez  
424 Sara, Roesland Gro Vatne, Rohlena Jakub, Rolo Anabela Pinto, Ropelle Eduardo R, Roshanravan  
425 Baback, Rossignol Rodrigue, Rossiter Harry B, Rousar Tomas, Rubelj Ivica, Rybacka-Mossakowska  
426 Joanna, Saada Reisch Ann, Safaei Zahra, Salin Karine, Salvadego Desy, Sandi Carmen, Saner Nicholas,  
427 Santos Diana, Sanz Alberto, Sardao Vilma, Sarlak Saharnaz, Sazanov Leonid A, Scaife Paula, Scatena  
428 Roberto, Schartner Melanie, Scheibye-Knudsen Morten, Schilling Jan M, Schlattner Uwe, Schmitt  
429 Sabine, Schneider Gasser Edith Mariane, Schoenfeld Peter, Schots Pauke C, Schulz Rainer, Schwarzer  
430 Christoph, Scott Graham R, Selman Colin, Sendon Pamela Marie, Shabalina Irina G, Sharma Pushpa,  
431 Sharma Vipin, Shevchuk Igor, Shirazi Reza, Shiroma Jonathan G, Siewiera Karolina, Silber Ariel M,  
432 Silva Ana Maria, Sims Carrie A, Singer Dominique, Singh Brijesh Kumar, Skolik Robert A, Smenes  
433 Benedikte Therese, Smith James, Soares Felix Alexandre Antunes, Sobotka Ondrej, Sokolova Inna,  
434 Solesio Maria E, Soliz Jorge, Sommer Natascha, Sonkar Vijay K, Sova Marina, Sowton Alice P,  
435 Sparagna Genevieve C, Sparks Lauren M, Spinazzi Marco, Stankova Pavla, Starr Jonathan, Stary Creed,  
436 Stelfa Gundega, Stepto Nigel K, Stevanovic Jelena, Stiban Johnny, Stier Antoine, Stocker Roland,  
437 Storder Julie, Sumbalova Zuzana, Suomalainen Anu, Suravajhala Prashanth, Svalbe Baiba, Swerdlow  
438 Russell H, Swiniuch Daria, Szabo Ildiko, Szewczyk Adam, Szibor Marten, Tanaka Masashi, Tandler  
439 Bernard, Tarnopolsky Mark A, Tausan Daniel, Tavernarakis Nektarios, Teodoro Joao Soeiro, Tepp  
440 Kersti, Thakkar Himani, Thapa Maheshwor, Thyfault John P, Tomar Dhanendra, Ton Riccardo, Torp  
441 May-Kristin, Towheed Atif, Treberg Jason R, Tretter Laszlo, Trewin Adam J, Trifunovic Aleksandra,  
442 Trivigno Catherine, Tronstad Karl Johan, Trougakos Ioannis P, Truu Laura, Tuncay Erkan, Turan  
443 Belma, Tyrrell Daniel J, Urban Tomas, Urner Sofia, Valentine Joseph Marco, Van Bergen Nicole J, Van  
444 der Ende Miranda, Van Hove Johan, Varricchio Frederick, Vaupel Peter, Vella Joanna, Vendelin Marko,  
445 Vercesi Anibal E, Verdaguer Ignasi Bofill, Vernerova Andrea, Victor Victor Manuel, Vieira Ligo  
446 Teixeira Camila, Vidimce Josif, Viel Christian, Vieyra Adalberto, Vilks Karlis, Villena Josep A,



447 Vincent Vinnyfred, Vinogradov Andrey D, Viscomi Carlo, Vitorino Rui Miguel Pinheiro, Vlachaki  
448 Walker Julia, Vogt Sebastian, Volani Chiara, Volska Kristine, Votion Dominique-Marie, Vujacic-  
449 Mirski Ksenija, Wagner Brett A, Ward Marie Louise, Warnsmann Verena, Wasserman David H, Watala  
450 Cezary, Wei Yau-Huei, Weinberger Klaus M, Weissig Volkmar, Whitfield Jamie, Wickert Anika,  
451 Wieckowski Mariusz R, Wiesner Rudolf J, Williams Caroline M, Winwood-Smith Hugh, Wohlgemuth  
452 Stephanie E, Wohlwend Martin, Wolff Jonci Nikolai, Wrutniak-Cabello Chantal, Wuest Rob CI, Yokota  
453 Takashi, Zablocki Krzysztof, Zanon Alessandra, Zanou Nadege, Zaugg Kathrin, Zaugg Michael,  
454 Zdrzilova Lucie, Zhang Yong, Zhang Yizhu, Zikova Alena, Zischka Hans, Zorzano Antonio, Zujovic  
455 Tijana, Zvejniece Liga

Affiliations:

[https://www.bioenergetics-communications.org/index.php/BEC2020.1\\_doi10.26124bec2020-0001.v1](https://www.bioenergetics-communications.org/index.php/BEC2020.1_doi10.26124bec2020-0001.v1)

### 459 **Acknowledgements**

460 We thank Beno M for management assistance, and Rich PR for valuable discussions. This publication  
461 is based upon work from COST Action CA15203 MitoEAGLE, supported by COST (European  
462 Cooperation in Science and Technology), in cooperation with COST Actions CA16225 EU-  
463 CARDIOPROTECTION and CA17129 CardioRNA, and K-Regio project MitoFit funded by the  
464 Tyrolian Government.

### 466 **Author contributions**

467 This manuscript developed as an open invitation to scientists and students to join as coauthors in the  
468 bottom-up spirit of COST, based on a first draft written by the corresponding author, who integrated  
469 coauthor contributions in a sequence of Open Access versions. Coauthors contributed to the scope and  
470 quality of the manuscript, may have focused on a particular section, and are listed in alphabetical order.  
471 Coauthors confirm that they have read the final manuscript and agree to implement the  
472 recommendations into future manuscripts, presentations and teaching materials.

### 474 **Competing interests**

475 E.G. is founder and CEO of Oroboros Instruments, Innsbruck, Austria. The other authors declare no  
476 competing financial interests.

477  
478

479 **Tables**

480

481 **Table 1 | Coupling control states and rates, and residual oxygen consumption in**  
 482 **mitochondrial preparations.** Respiration- and phosphorylation-flux,  $J_{\text{kO}_2}$  and  $J_{\text{P}}$ , are rates,  
 483 characteristic of a state in conjunction with the protonmotive force,  $pmF$ . Coupling states are  
 484 established at kinetically-saturating concentrations of fuel substrates and  $\text{O}_2$ .  
 485

State	Rate	$J_{\text{kO}_2}$	$J_{\text{P}}$	$pmF$	Inducing factors	Limiting factors
LEAK	$L$	low, cation leak-dependent respiration	0	max.	back-flux of cations including proton leak, proton slip	$J_{\text{P}} = 0$ : (1) without ADP, $L(n)$ ; (2) max. ATP/ADP ratio, $L(T)$ ; or (3) inhibition of the phosphorylation-pathway, $L(O_{\text{my}})$
OXPHOS	$P$	high, ADP-stimulated respiration, OXPHOS-capacity	max.	high	kinetically-saturating [ADP] and $[\text{P}_i]$	$J_{\text{P}}$ by phosphorylation-pathway capacity; or $J_{\text{kO}_2}$ by ET-capacity
ET	$E$	max., noncoupled respiration, ET-capacity	0	low	optimal external uncoupler concentration for max. $J_{\text{O}_2, E}$	$J_{\text{kO}_2}$ by ET-capacity
ROX	$R_{\text{ox}}$	min., residual $\text{O}_2$ consumption	0	0	$J_{\text{O}_2, R_{\text{ox}}}$ in non-ET-pathway oxidation reactions	inhibition of all ET-pathways; or absence of fuel substrates

486

487  
488**Table 2 | Terms on respiratory coupling and uncoupling**

Term	$J_{kO_2}$	$P \gg O_2$	Notes	
intrinsic, no protonophore added	uncoupled	$L$	0	non-phosphorylating <b>LEAK-respiration</b> (Fig. 2)
	proton leak-uncoupled		0	component of $L$ , $H^+$ diffusion across the mtIM (Fig. 2b-d)
	inducibly uncoupled		0	by UCP1 or cation ( <i>e.g.</i> , $Ca^{2+}$ ) cycling; strongly stimulated by permeability transition (mtPT); experimentally induced by valinomycin in the presence of $K^+$
	decoupled		0	component of $L$ , proton slip when protons are effectively not pumped in the redox proton pumps CI, CIII and CIV or are not driving phosphorylation (F-ATPase) <sup>25</sup> (Fig. 2b-d)
	loosely coupled		0	component of $L$ , lower coupling due to superoxide formation and bypass of proton pumps by electron leak with univalent reduction of $O_2$ to superoxide ( $O_2^{\cdot-}$ ; superoxide anion radical)
	dyscoupled		0	mitochondrial dysfunction due to pathologically, toxicologically, environmentally increased uncoupling
noncoupled	$E$		0	ET-capacity, non-phosphorylating respiration stimulated to maximum flux at optimum exogenous protonophore concentration (Fig. 2d)
well-coupled	$P$		high	<b>OXPPOS-capacity</b> , phosphorylating respiration with an intrinsic LEAK component (Fig. 2c)
fully coupled	$P - L$		max.	<b>OXPPOS-capacity</b> corrected for LEAK-respiration (Fig. 2a)
acoupled			0	electron transfer in mitochondrial fragments without vectorial proton translocation upon loss of vesicular (compartmental) integrity

489  
490

491 **Table 3 | Conversion of units**

492 **a.** Conversion of  $O_2$  flow,  $I_{O_2}$ , to SI units ( $e^-$  is the number of electrons or reducing  
 493 equivalents)

1 Unit		Multiplication factor	SI-unit
ng.atom $O \cdot s^{-1}$	(2 $e^-$ )	0.5	nmol $O_2 \cdot s^{-1}$
ng.atom $O \cdot \text{min}^{-1}$	(2 $e^-$ )	8.33	pmol $O_2 \cdot s^{-1}$
natom $O \cdot \text{min}^{-1}$	(2 $e^-$ )	8.33	pmol $O_2 \cdot s^{-1}$
nmol $O_2 \cdot \text{min}^{-1}$	(4 $e^-$ )	16.67	pmol $O_2 \cdot s^{-1}$
nmol $O_2 \cdot h^{-1}$	(4 $e^-$ )	0.2778	pmol $O_2 \cdot s^{-1}$

494

495 **b.** Conversion of units with preservation of numerical values  
 496

Name	Frequently used unit	Equivalent unit	Notes
volume-specific flux, $J_{V,O_2}$	pmol·s <sup>-1</sup> ·mL <sup>-1</sup>	nmol·s <sup>-1</sup> ·L <sup>-1</sup>	1
	mmol·s <sup>-1</sup> ·L <sup>-1</sup>	mol·s <sup>-1</sup> ·m <sup>-3</sup>	
cell-specific flow, $I_{O_2/N_{ce}}$	pmol·s <sup>-1</sup> ·10 <sup>-6</sup> cells	amol·s <sup>-1</sup> ·cell <sup>-1</sup>	2
	pmol·s <sup>-1</sup> ·10 <sup>-9</sup> cells	zmol·s <sup>-1</sup> ·cell <sup>-1</sup>	3
cell number concentration, $C_{N_{ce}}$	10 <sup>6</sup> cells·mL <sup>-1</sup>	10 <sup>9</sup> cells·L <sup>-1</sup>	
mitochondrial protein concentration, $C_{mtE}$	0.1 mg·mL <sup>-1</sup>	0.1 g·L <sup>-1</sup>	
mass-specific flux, $J_{O_2/m}$	pmol·s <sup>-1</sup> ·mg <sup>-1</sup>	nmol·s <sup>-1</sup> ·g <sup>-1</sup>	4
volume	1,000 L	m <sup>3</sup> (1,000 kg)	
	L	dm <sup>3</sup> (kg)	
	mL	cm <sup>3</sup> (g)	
	μL	mm <sup>3</sup> (mg)	
	fL	μm <sup>3</sup> (pg)	5
amount of substance concentration	M = mol·L <sup>-1</sup>	mol·dm <sup>-3</sup>	

497 1 pmol: picomole = 10<sup>-12</sup> mol4 nmol: nanomole = 10<sup>-9</sup> mol498 2 amol: attomole = 10<sup>-18</sup> mol5 fL: femtolitre = 10<sup>-15</sup> L499 3 zmol: zeptomole = 10<sup>-21</sup> mol

500

**Table 4 | Terms, symbols, and units.** SI base units are used, except for the liter [L = dm<sup>3</sup>]

Term	Symbol	Unit	Links and comments
alternative quinol oxidase	AOX		Fig. 1b
adenosine diphosphate	ADP		Tab. 1; Fig. 1 and 2
adenosine triphosphate	ATP		Tab. 1; Fig. 1 and 2
ATP hydrolysis ATP→ADP	P <sub>«</sub>		Fig. 2b,c
catabolic reaction	k		Tab. 1 and 2; Fig. 1 and 2
catabolic respiration	$J_{kO_2}$	<i>varies</i>	Fig 1c, Fig. 2b-d
cell concentration (number [x])	$C_{Nce}$	[x·L <sup>-1</sup> ]	for normalization of rate
coenzyme Q-junction	Q-junction		Fig. 1b
electron transfer Complexes	CI to CIV		Fig. 1b; F <sub>1</sub> F <sub>0</sub> -ATPase is not an ET- but a phosphorylation-pathway Complex, hence the term Complex V should not be used
electron transfer, state	ET		Tab. 1; Fig. 2a (State 3u)
electron transfer system	ETS		Fig. 1b
ET-capacity	$E$	<i>varies</i>	Tab. 1; Fig. 2a,d; rate
ET-excess capacity	$E-P$	<i>varies</i>	Fig. 2a
flow	$I$	[mol·s <sup>-1</sup> ]	Fig. 3; extensive quantity
flux	$J$	<i>varies</i>	Fig. 3; size-specific quantity
inorganic phosphate	P <sub>i</sub>		Fig. 1d
inorganic phosphate carrier	PiC		Fig. 1d
LEAK-state	<b>LEAK</b>		Tab. 1; Fig. 2a (compare State 4)
LEAK-respiration	$L$	<i>varies</i>	rate; Tab. 1; Fig. 2a,b
mass of sample or object $X$	$m_X$ or $m_{NX}$	[kg] or [kg·x <sup>-1</sup> ]	Fig. 3
mass, dry mass	$m_d$	[kg] or [kg·x <sup>-1</sup> ]	(dry weight)
mass, wet mass	$m_w$	[kg] or [kg·x <sup>-1</sup> ]	(wet weight)
mitochondria or mitochondrial	mt		compare mtDNA
mitochondrial elementary marker	$mtE$	[mtEU]	Fig. 3; quantity of mt-marker
mitochondrial elementary unit	mtEU	<i>varies</i>	Fig. 3; specific units for mt-marker
mitochondrial inner membrane	mtIM		Fig. 1 (MIM)
mitochondrial outer membrane	mtOM		Fig. 1 (MOM)
NADH-junction	N-junction		Fig. 1b
number concentration of $X$	$C_{NX}$	[x·L <sup>-1</sup> ]	for normalization of rate
number format	$\underline{N}$	[x]	Fig. 3
number of cells	$N_{ce}$	[x]	for normalization of rate
number of entities $X$	$N_X$	[x]	Fig. 3; for normalization of rate
O <sub>2</sub> concentration	$c_{O_2} = n_{O_2} \cdot V^{-1}$	[mol·L <sup>-1</sup> ]	[O <sub>2</sub> ]
O <sub>2</sub> flow per countable object	$I_{O_2/NX}$	[mol·s <sup>-1</sup> ·x <sup>-1</sup> ]	Fig. 3
O <sub>2</sub> flow per chamber	$I_{O_2}$	[mol·s <sup>-1</sup> ]	Fig. 3
O <sub>2</sub> flux, in reaction r	$J_{rO_2}$	<i>varies</i>	Fig. 1a
O <sub>2</sub> flux, volume-specific	$J_{V,O_2}$	[mol·s <sup>-1</sup> ·L <sup>-1</sup> ]	Fig. 3; per volume of chamber
O <sub>2</sub> flux, sample mass-specific	$J_{O_2/mX}$	[mol·s <sup>-1</sup> ·kg <sup>-1</sup> ]	Fig. 3; specify dry or wet mass
oxidative phosphorylation	OXPHOS		Fig. 1
OXPHOS-state	<b>OXPHOS</b>		Tab. 1; Fig. 2a (State 3 at kinetically-saturating [ADP] and [P <sub>i</sub> ])
OXPHOS-capacity	$P$	<i>varies</i>	rate; Tab. 1; Fig. 2a,c
permeability transition	mtPT		Tab. 2; MPT is widely used
phosphorylation flux ADP→ATP	$J_{P_{»}}$	<i>varies</i>	Fig. 2b-d
phosphorylation of ADP to ATP	P <sub>»</sub>		Fig. 1
P <sub>»</sub> /O <sub>2</sub> ratio	P <sub>»</sub> /O <sub>2</sub>		mechanistic $Y_{P_{»}/O_2}$ , calculated from pump stoichiometries; Fig. 1c



558	proton in the negative compartment	$H^+_{\text{neg}}$		Fig. 2b-d
559	proton in the positive compartment	$H^+_{\text{pos}}$		Fig. 1b,c; Fig. 2b-d
560	protonmotive flux to the negative			
561	compartment	$J_{\text{mH}^+\text{neg}}$	<i>varies</i>	Fig. 2d,f
562	protonmotive flux to the positive			
563	compartment	$J_{\text{mH}^+\text{pos}}$	<i>varies</i>	Fig. 2b,c,d
564	protonmotive force	$pmF$	[V]	Figures 1, 2A and 4; Table 1
565	rate of electron transfer in ET-state	$E$	<i>varies</i>	Tab. 1; ET-capacity
566	rate of LEAK-respiration	$L$	<i>varies</i>	Tab. 1; $L(n)$ , $L(T)$ , $L(O_{\text{my}})$
567	rate of oxidative phosphorylation	$P$	<i>varies</i>	Tab. 1; OXPHOS-capacity
568	rate of residual oxygen consumption	$R_{ox}$	<i>varies</i>	Tab. 1
569	residual oxygen consumption, state	ROX		Tab. 1
570	sample type	$X$		
571	substrate-uncoupler-inhibitor-			
572	titration protocol	SUIT		
573	tricarboxylic acid cycle	TCA cycle		Fig. 1a
574	volume	$V$	[L]	
575	volume format	$\underline{V}$	[L]	Fig. 3
576	volume of sample or object $X$	$V_X$ or $V_{\underline{M}X}$	[L] or $[L \cdot x^{-1}]$	Fig. 3
577				
578				

---

579 **Figures**

580

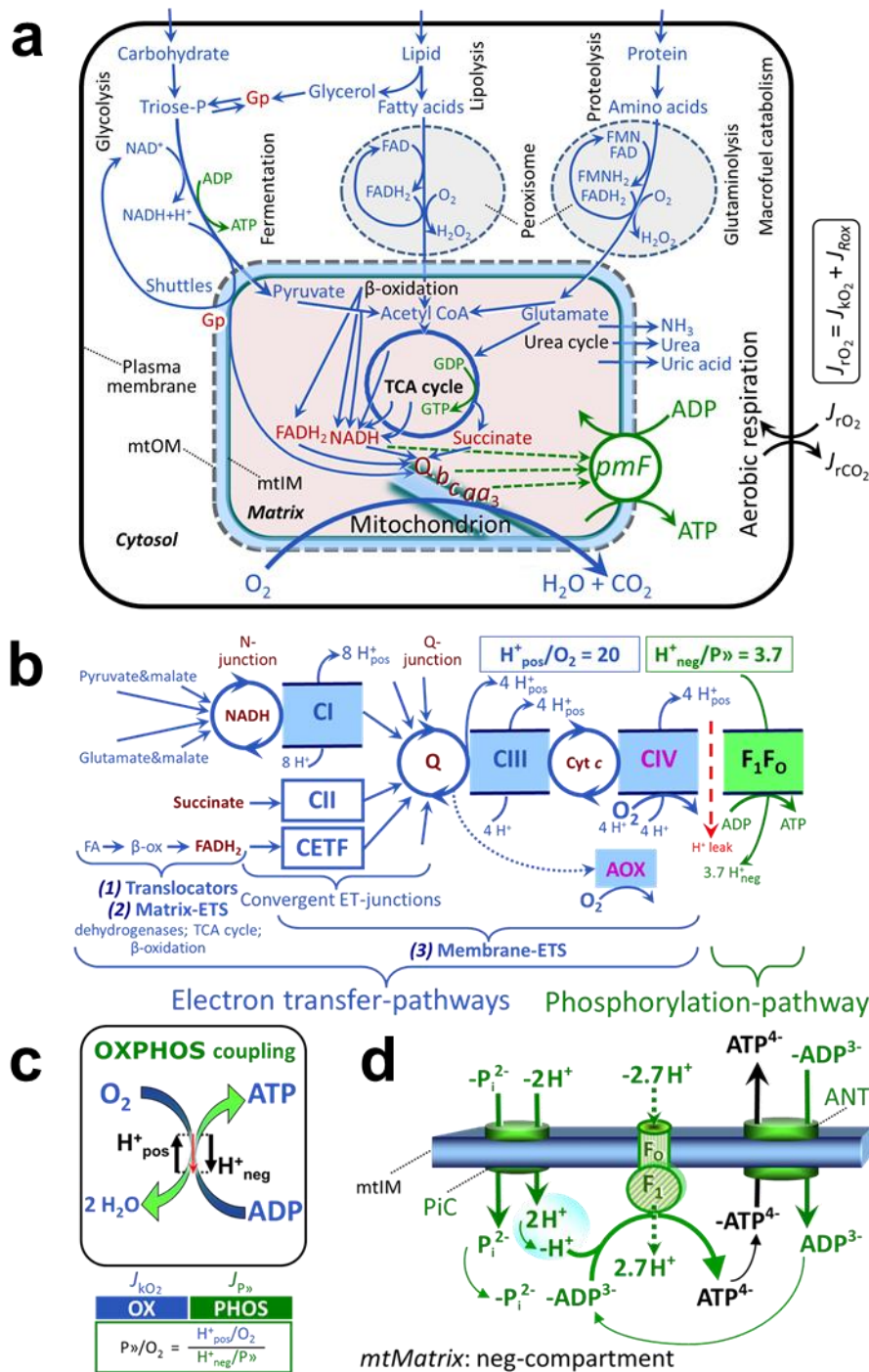
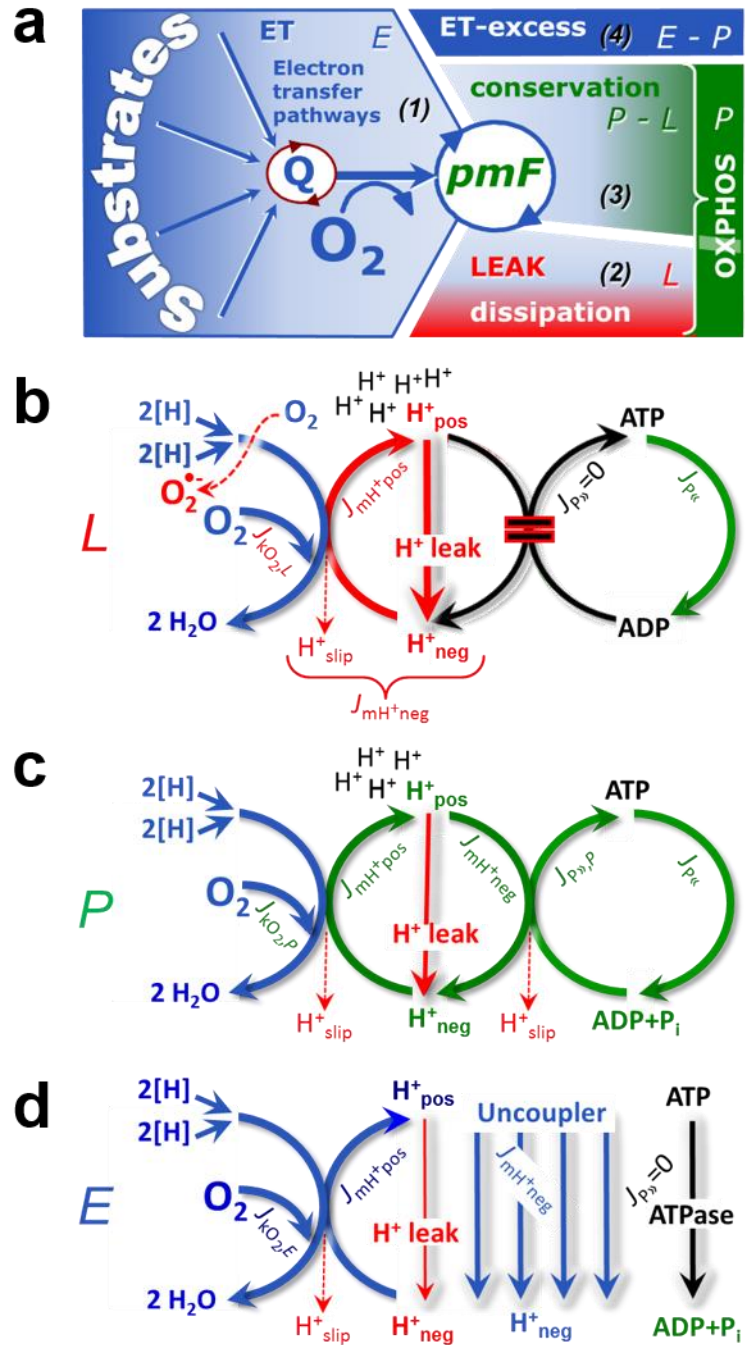


**Fig. 1. | Respiration and oxidative phosphorylation (OXPHOS).** (a) Cell respiration: uptake of small molecules and catabolism of macronutrients provide the mitochondrial fuel substrates (electron donors), which are oxidized with electron transfer to O<sub>2</sub> (electron acceptor). Dashed arrows indicate the connection between the redox proton pumps (respiratory Complexes CI, CIII and CIV) and the transmembrane protonmotive force, *pmF*. Coenzyme Q (Q) and the cytochromes *b*, *c*, and *aa<sub>3</sub>* are redox systems of the mitochondrial inner membrane, mtIM. Glycerol-3-phosphate, Gp. (b) Mitochondrial respiration: The mitochondrial electron transfer system (ETS) is (1) fueled by diffusion and transport of substrates across the mitochondrial outer and inner membranes (mtOM and mtIM), and in addition consists of the (2) matrix-ETS, and (3) membrane-ETS. Electron transfer converges from dehydrogenases at the NADH-junction (N-junction), and from CI,

581  
582  
583  
584  
585  
586  
587  
588  
589  
590  
591  
592

593 CII and electron transferring flavoprotein complex (CETF) at the Coenzyme Q-junction  
594 (Q-junction). Unlabeled arrows converging at the Q-junction indicate additional ETS-  
595 sections with electron entry into Q through Gp-dehydrogenase, dihydroorotate  
596 dehydrogenase, proline dehydrogenase, choline dehydrogenase, and sulfide-ubiquinone  
597 oxidoreductase. The dotted arrow indicates the branched pathway of oxygen consumption  
598 by alternative quinol oxidase (AOX). ET-pathways are coupled to the phosphorylation-  
599 pathway. The  $H^+_{\text{pos}}/O_2$  ratio is the outward proton flux from the matrix space to the  
600 positively (pos) charged vesicular compartment, divided by catabolic  $O_2$  flux in the NADH-  
601 pathway <sup>26</sup>. The  $H^+_{\text{neg}}/P_{\gg}$  ratio is the inward proton flux from the inter-membrane space to  
602 the negatively (neg) charged matrix space, divided by phosphorylation flux of ADP to ATP.  
603 These stoichiometries are not fixed because of ion leaks and proton slip. Modified from ref  
604 27. **(c) OXPHOS-coupling:** The  $H^+$  circuit couples  $O_2$  flux through the catabolic ET-  
605 pathway,  $J_{kO_2}$ , to flux through the phosphorylation-pathway of ADP to ATP,  $J_{P_{\gg}}$ .  
606 **(d) Phosphorylation-pathway:** the proton pump  $F_1F_0$ -ATPase (F-ATPase, ATP synthase),  
607 adenine nucleotide translocase (ANT), and inorganic phosphate carrier (PiC). The  $H^+_{\text{neg}}/P_{\gg}$   
608 stoichiometry is the sum of the coupling stoichiometry in the F-ATPase reaction ( $-2.7 H^+_{\text{pos}}$   
609 from the positive intermembrane space,  $2.7 H^+_{\text{neg}}$  to the matrix, *i.e.*, the negative  
610 compartment) and the proton balance in the translocation of  $ADP^{3-}$ ,  $ATP^{4-}$  and  $P_i^{2-}$  (negative  
611 for substrates) <sup>12</sup>. Modified from ref 8.  
612

613 **Fig. 2 | Respiratory states and**  
 614 **rates. (a)** Four-compartment model  
 615 of oxidative phosphorylation:  
 616 respiratory states (ET, OXPHOS,  
 617 LEAK) and corresponding rates ( $E$ ,  
 618  $P$ ,  $L$ ) are connected by the  
 619 protonmotive force,  $pmF$ . (1) ET-  
 620 capacity,  $E$ , is partitioned into (2)  
 621 dissipative LEAK-respiration,  $L$ ,  
 622 when the Gibbs energy change of  
 623 catabolic  $O_2$  flux is irreversibly lost,  
 624 (3) net OXPHOS-capacity,  $P-L$ , with  
 625 partial conservation of the capacity  
 626 to perform work, and (4) the ET-  
 627 excess capacity,  $E-P$ . (b) **LEAK-**  
 628 **rate,  $L$** : Oxidation only, since  
 629 phosphorylation is arrested,  $J_{P_{\gg}} = 0$ ,  
 630 and catabolic  $O_2$  flux,  $J_{kO_2,L}$ , is  
 631 controlled mainly by the proton  
 632 leak and slip,  $J_{mH^{+neg}}$  (motive,  
 633 subscript m), at maximum  
 634 protonmotive force. ATP may be  
 635 hydrolyzed by ATPases,  $J_{P_{\ll}}$ ; then  
 636 phosphorylation must be blocked.  
 637 (c) **OXPHOS-rate,  $P$** : Oxidation  
 638 coupled to phosphorylation,  $J_{P_{\gg}}$ ,  
 639 which is stimulated by  
 640 kinetically-saturating [ADP] and  
 641 [ $P_i$ ], supported by a high  
 642 protonmotive force maintained  
 643 by pumping of protons to the  
 644 positive compartment,  $J_{mH^{+pos}}$ .  $O_2$   
 645 flux,  $J_{kO_2,P}$ , is well-coupled at a  
 646  $P_{\gg}/O_2$  flux ratio of  $J_{P_{\gg,P}}/J_{O_2,P}$ .  
 647 Extramitochondrial ATPases may  
 648 recycle ATP,  $J_{P_{\ll}}$ . (d) **ET- rate,  $E$** :  
 649 Oxidation only, since  
 650 phosphorylation is zero,  $J_{P_{\gg}} = 0$ ,  
 651 at optimum exogenous uncoupler  
 652 concentration when noncoupled  
 653 respiration,  $J_{kO_2,E}$ , is maximum.  
 654 Modified from ref 8.  
 655



The F-ATPase may hydrolyze extramitochondrial ATP.

656 **Fig. 3 | Different meanings of**  
 657 **rate: flow and flux dependent on**  
 658 **normalization for sample or**  
 659 **instrumental chamber.**

660 Fundamental distinction between  
 661 metabolic rate related to the  
 662 experimental sample (left) or to  
 663 the instrumental chamber (right).  
 664 Left: Results are expressed as  
 665 mass-specific *flux*,  $J_{mX}$ , per mg  
 666 protein, dry or wet mass. Cell  
 667 volume,  $V_{ce}$ , may be used for  
 668 normalization (volume-specific  
 669 flux,  $J_{Vce}$ ). Normalization per  
 670 mitochondrial elementary marker,  
 671 *mtE*, relies on determination of mt-  
 672 markers expressed in various  
 673 mitochondrial elementary units [mtEU]. Right: Flow per instrumental chamber,  $I$ , or flux per chamber  
 674 volume,  $J_V$ , are reported for methodological reasons.  
 675

